

Title page

UDP-Glucuronic Acid Binds First and the Aglycone Substrate Binds Second to Form a Ternary Complex in UGT1A9-Catalyzed Reactions, in Both the Presence and Absence of BSA

Nenad Manevski, Jari Yli-Kauhaluoma and Moshe Finel

Division of Pharmaceutical Chemistry (N.M. and J.Y.-K.), and Centre for Drug Research (N.M., and M.F.), Faculty of Pharmacy, University of Helsinki, Helsinki, Finland

DMD #47746

Running title page

Running title: Enzyme kinetics of UGT1A9 in the presence of BSA

Corresponding author: Dr. Moshe Finel, Centre for Drug Research, Faculty of Pharmacy,
P.O. Box 56 (Viikinkaari 5), FI-00014 University of Helsinki, Finland

E-mail: Moshe.Finel@helsinki.fi, Fax: +358 9 191 59556

Manuscript statistics:

Number of text pages: 40

Number of tables: 5

Number of figures: 8

Number of references: 41

Number of words in the Abstract: 241

Number of words in the Introduction: 742

Number of words in the Discussion: 1577

Abbreviations:

BSA, bovine serum albumin; CI, confidence interval of the mean; Eq., equation; 4-MU, 4-methylumbelliferone; 4-MUG, 4-methylumbelliferone- β -D-glucuronide; RED, rapid equilibrium dialysis; UDPGA, UDP- α -D-glucuronic acid; UGT, UDP-glucuronosyltransferase.

Abstract

The presence of bovine serum albumin (BSA) largely modulates the enzyme kinetics parameters of the human UDP-glucuronosyltransferase (UGT) 1A9, increasing both the apparent aglycone substrate affinity of the enzyme and its limiting reaction velocity (Manevski *et al.*, Drug Metabol. Dispos. 39:2117–2129, 2011). For better understanding of the BSA effects and examining whether or not its presence changes the catalytic mechanism, we have studied the enzyme kinetics of 4-methylumbelliferone (4-MU) glucuronidation by UGT1A9 in the presence and absence of 0.1% BSA, using bisubstrate enzyme kinetic experiments, in both the forward and reverse directions, as well as product and dead-end inhibition. The combined results strongly suggest that the reaction mechanism of UGT1A9 and, presumably, other human UGTs as well, involves the formation of a compulsory-order ternary-complex, with UDPGA as the first binding substrate. Based on the enzyme kinetic parameters measured for the forward and reverse reactions, the equilibrium constant of the overall reaction was calculated ($K_{eq} = 574$) and the relative magnitudes of the reaction rate constants were elucidated. The inclusion of BSA in the bisubstrate kinetic experiments quantitatively changed the apparent enzyme kinetic parameters, presumably by removing internal inhibitors that bind to the binary E•UDPGA complex, as well as to the ternary E•UDPGA•aglycone complex. Nevertheless, the underlying compulsory-order ternary-complex mechanism with UDPGA binding first is the same in both the absence and presence of BSA. The results offer novel understanding of UGT enzyme kinetic mechanism and BSA effects.

Introduction

Human UDP-glucuronosyltransferases (UGTs) transfer the glucuronic acid moiety from UDP- α -D-glucuronic acid (UDPGA) to nucleophilic groups on small organic molecules of both endo- and xenobiotic origin (Bock, 2010, Miners et al., 2010). The conjugation with glucuronic acid increases the hydrophilicity of the original aglycone substrate and stimulates excretion from the cell, probably by facilitating molecular recognition by efflux transporters (Jemnitz et al., 2010). The amino acid sequences of individual UGT enzymes are highly homologous (Mackenzie et al., 2005), and the enzymes exhibit distinct but partially overlapping substrates and inhibitors specificity (Miners et al., 2010). The UGTs are variably expressed in human tissues, particularly in the liver, intestine, and kidneys (Court et al., 2012, Ohno and Nakajin, 2009). The enzyme at the focus of this study, UGT1A9, is important in the metabolic elimination of several therapeutic drugs, including entacapone (Lautala et al., 2000), propofol (Soars et al., 2004), and mycophenolic acid (Bernard and Guillemette, 2004), and is highly expressed in liver and kidneys (Court et al., 2012).

The presence of purified bovine serum albumin (BSA) in the glucuronidation reaction greatly enhances the *in vitro* activity of the human UGT1A9; regardless of whether recombinant enzyme or human liver microsomes (HLM) are used as the enzyme source (Manevski et al., 2011). The inclusion of BSA in both the entacapone and 4-methylumbelliferone (4-MU) glucuronidation assays decreased the K_m values, increased the V_{max} values, and led to some changes in the enzyme kinetic model (Manevski et al., 2011). Such changes in enzyme kinetics open many questions, both practical and theoretical. Two of the more challenging questions are what is the underlying mechanism of the BSA effects and are the results of earlier studies on the UGTs' reaction mechanism—performed in the absence of BSA—also valid in the presence of this modulator.

The previously suggested BSA-mediated removal of competitive inhibitors, perhaps fatty acids that are released upon cell disruption, could account for the observed K_m decrease that was found in UGT2B7 (Rowland et al., 2007, Rowland et al., 2008). Nevertheless, the removal of competitive inhibitors could not explain the V_{max} increase or the changes in the enzyme kinetic model that we found in UGT1A9 (Manevski et al., 2011). To account for the latter observations, we proposed that BSA also removes inhibitors that are not directly competing with aglycone substrate binding (Manevski et al., 2011). Such a hypothesis, however, is poorly defined without knowledge of the reaction mechanism, particularly in enzymes, like the UGTs, that catalyze a two-substrate two-product reaction.

The UGTs reaction mechanism has been studied extensively in the last 40 years, yielding variable results (Table 1). Many of these studies found that, regardless of enzyme source and experimental conditions, UGT-catalyzed reactions follow ternary-complex mechanism. The formation of ternary-complex is also supported by the evidence that the glucuronidation reaction resembles S_N2 -type nucleophilic substitution reaction, with the inversion of the glucuronic acid anomeric carbon from α - in UDPGA to β -configuration in the formed glucuronide (Axelrod et al., 1958, Johnson and Fenselau, 1978). Alongside the broad agreement on the formation of ternary complex, however, there is disagreement among the previous studies on whether or not the two substrates, the aglycone substrate and the UDPGA, bind in a random order or in a compulsory order (Table 1). The observed discrepancies in the order of substrate binding may have arisen from the use of liver microsomal preparations that contain multiple UGT enzymes (Potrepka and Spratt, 1972, Vessey and Zakim, 1972, Sanchez and Tephly, 1975, Rao et al., 1976, Koster and Noordhoek, 1983), or of partially purified UGT enzymes (Matern et al., 1982, Matern et al., 1982, Falany et al., 1987, Yin et al., 1994) that may have been inactivated by detergents during the purification process (Kurkela et al., 2003).

A previous study from this laboratory, that was performed using individual recombinant UGT enzymes of subfamily 1A, concluded that UDPGA is the first binding substrate (Luukkanen et al., 2005). That study was carried out in the absence of BSA and focused on UGT1A9, an enzyme we recently found to be highly affected by the presence of BSA (Manevski et al., 2011). Due to this, it is particularly interesting to examine whether or not the presence of BSA affects the reaction mechanism of UGT1A9. In order to address this question, we have carried out the detailed study that is described below. The results provide comprehensive insights into the UGT reaction mechanism, as well as a theoretical framework for future mechanistic studies with recombinant UGTs.

Materials and Methods

Compounds and reagents. 4-MU (>99.0%, CAS 90-33-5), 1-naphthol (>99%, CAS 90-15-3), UDPGA (ammonium salt, 98–100%, CAS 43195-60-4), UDP (disodium salt hydrate, $\geq 96\%$, CAS 27821-45-0), 4-methylumbelliferone- β -D-glucuronide (4-MUG, $\geq 98\%$, CAS 6160-80-1), 1-naphthol- β -D-glucuronide (>99%, CAS 83833-12-9), sodium phosphate monobasic dihydrate ($\geq 99\%$, CAS 13472-35-0), and bovine serum albumin (BSA, $\geq 96\%$, CAS 9048-46-8, essentially fatty acid free, $\leq 0.004\%$) were purchased from Sigma-Aldrich (St. Louis, MO, USA). Magnesium chloride hexahydrate and perchloric acid were obtained from Merck (Darmstadt, Germany). Formic acid (98–100%) was from Riedel-deHaën (Seelze, Germany). Disodium hydrogen phosphate dihydrate was purchased from Fluka (Buchs, Switzerland). Liquid chromatography–mass spectrometry-grade solvents were used throughout the study.

Recombinant UGT1A9 and negative control membranes. Recombinant human UGT1A9 was expressed, as His-tagged protein, in baculovirus-infected *Sf9* insect cells (Kurkela et al., 2007). Negative control membranes, called "Bac control", were prepared from insect cells that were infected with a modified baculovirus that does not encode any functional UGT. Protein concentration in the UGT1A9-enriched and "Bac control" membranes was determined by the BCA method (Pierce Biotechnology, Rockford, IL, USA).

Substrate binding assays. The binding of entacapone, 4-MU, and 1-naphthol to 0.1% and 1% BSA, as well as to insect cells membranes, the "Bac control" membranes, was measured in this study by the rapid equilibrium dialysis system (RED, Thermo Scientific, Rockford, IL, USA). The system consisted of reusable Teflon[®] base plate and single-use device insets comprised of two side-by-side vertical cylinder chambers separated by dialysis membrane (molecular weight cut-off value ~ 8000 Da). The RED device insets were placed into the base plate and the sample chamber was filled with 400 μ L of the test compound solution in 50 mM phosphate

buffer (pH 7.4) that also contained the “binding” macromolecules, 0.1%, 1% BSA or insect cell membranes (0.02–0.2 mg/mL of total membrane protein). The buffer chamber was filled only with 600 μ L of blank buffer, 50 mM phosphate buffer (pH 7.4), without the test compound and the binding macromolecule. The filled up RED device was covered with Parafilm[®] and incubated at 100 rpm at 37 °C for 6 to 8 h. The test compounds concentration range in the sample chamber was 5–750 μ M, 5–500 μ M and 0.05–5 μ M for entacapone, 4-MU, and 1-naphthol, respectively. Following incubation, a 50 μ L aliquot from each chamber was mixed with 100 μ L of ice-cold 4 M perchloric acid/methanol (1:5 mix), placed at –18 °C for 30 min, centrifuged (at room temperature) for 5 min at 16000g and the test compound concentration in the resulting supernatant was determined by HPLC analyses. The unbound fraction of the test compound, f_u , was calculated using the equation: $f_u = \frac{[S]_{buffer\ chamber}}{[S]_{sample\ chamber}}$, where $[S]_{buffer\ chamber}$ and $[S]_{sample\ chamber}$ are the concentrations of the test compound in the respective chambers at the end of the incubation.

Glucuronidation assays. Stock solutions of 4-MU, 4-methylumbelliferone- β -D-glucuronide (4-MUG), and 1-naphthol were prepared in methanol and diluted with methanol to the desired concentrations immediately before use. Appropriate amounts of these dilutions were transferred into 1.5 mL bench-top centrifuge tubes and the solvent was evaporated *in vacuo* at ambient temperature. The solid residues were dissolved in the reaction mixture that was composed of phosphate buffer (50 mM, pH 7.4), MgCl₂ (10 mM), BSA (zero or 0.1%), and the enzyme source (0.02–0.2 mg/mL of total membrane protein, either UGT1A9-enriched or "Bac control" membranes), to a final volume of 100 μ L. The concentration of MgCl₂ required for optimal UGT1A9 activity was selected based on literature data (Walsky et al., 2012). Alamethicin was not added since it does not significantly stimulate the glucuronidation

activity of recombinant UGT enzymes expressed in *Sf9* insect cells (Walsky et al., 2012, Zhang et al., 2011, Kaivosari et al., 2008).

The reaction mixtures, with the dissolved aglycone substrate, were incubated first for 20 min at room temperature and then at 37°C for 5 min. The glucuronidation reaction was initiated by the addition of UDPGA (to a final concentration of 20–5000 µM), and carried out, protected from light, at 37°C for 15–60 min, depending on the substrate consumption rate. The reactions in the reverse direction were initiated by the addition of UDP to a final concentration of 5–1000 µM. Negative controls, including incubations in the absence of UDPGA (or UDP), without substrate, or with the “Bac-control” insect cells membranes instead of the UGT1A9-enriched membranes and in the presence of both substrates, were carried out for each set of assays. The glucuronidation reactions in the forward direction were terminated by the addition of 60 µL ice-cold 4 M perchloric acid/methanol (1:5). To minimize the risk of non-enzymatic glucuronide hydrolysis, the reactions in the reverse direction were terminated by the addition of 100 µL ice-cold 5% acetic acid in methanol. Following reaction termination, the tubes were transferred to –20 °C for 60 min and then centrifuged at 16000g for 5 min at room temperature. Aliquots of the resulting supernatants were transferred to dark glass vials and subjected to HPLC analyses.

Analytical methods. The HPLC system consisted of an Agilent 1100 series degasser, binary pump, 100-vial autosampler, thermostated column compartment, multiple wavelengths UV detector, and fluorescence detector (Agilent Technologies, Palo Alto, CA, USA). A Poroshell 120 EC-C18 column (4.6 × 100 mm, 2.7 µm; Agilent Technologies, Palo Alto, CA, USA), was used for all the separations, at column temperature of 40°C and an eluent flow rate of 1 mL/min. The resulting chromatograms were analyzed with Agilent ChemStation software (rev.

B.01.01) on Windows XP Professional. Further details of the analytical methods and analyte quantification are presented in Table 2.

Enzyme kinetic assays and data analysis. The protein concentrations and incubation times for the kinetic analyses reactions were selected based on preliminary assays so that no more than 10% of the substrate is consumed during the incubation. In the case of bisubstrate enzyme kinetics and inhibition assays, we performed a number of optimization assays in order to select the suitable concentrations of substrates and inhibitors, as well as protein concentration, incubation time and optimal parameters of the analytical method for the final assays. Initial velocity measurements in the enzyme kinetic assays in which a concentration of a single substrate was varied were performed in triplicates and are presented as the average \pm S.E. Initial velocity measurements for the bisubstrate enzyme kinetics and the inhibition studies were performed in duplicates and are presented as the average value (the variation between two parallel samples in these experiments was not more than 15%, but the differences between the duplicates were much lower than this in most cases). The lines in the Eadie-Hofstee and Lineweaver-Burk plots were plotted with enzyme kinetic parameters obtained from the curve fittings, not by linear regression. Although Eadie-Hofstee plots offer a more reliable presentation of the enzyme kinetics data (Dowd and Riggs, 1965), due to the widespread use of the Lineweaver-Burk “double-reciprocal” plots, we have used them to visualize the outcome of product and dead-end inhibition studies. The bisubstrate experiments initial rates for the forward reaction catalyzed by the recombinant UGT1A9 were determined by varying the concentration of both substrates simultaneously: the sugar acid donor UDPGA (20–2000 μ M) and the aglycone substrate (1–50 and 1–180 μ M, with and without substrate inhibition, respectively). The initial rates in the bisubstrate reverse reactions were measured by simultaneously varying the concentration of UDP (5–1000 μ M) and 4-MUG (150–10000 μ M). The incubation times were varied from 10 to 60 min. The enzyme kinetic parameters were

obtained by fitting the kinetic models to the experimental data, using GraphPad Prism version 5.04 for Windows (GraphPad Software Inc., San Diego, CA, USA). The best (most appropriate for each reaction) kinetic model was selected based on visual inspection of the Eadie-Hofstee and Lineweaver-Burk plots, residuals graphs, parameter S.E. and 95% confidence intervals estimates (95% CI), the calculated r^2 values, and the corrected Akaike's information criterion. In assays containing BSA, the free substrate or inhibitor concentrations (f_u , or fraction unbound), were corrected according to the measured drug binding to BSA under the specific conditions of each glucuronidation assay (see *Drug binding assays* above). The initial glucuronidation velocities in the single substrate enzyme kinetics assays were fitted to the following equations:

Michaelis-Menten model:

$$(1) v = \frac{v_{max}[S]}{K_m + [S]}$$

Where v is the initial velocity of the reaction, $[S]$ is the substrate concentration, V_{max} is the limiting velocity at saturating concentration of substrate, and K_m is the Michaelis-Menten constant (concentration of substrate at 0.5 of V_{max}).

Substrate inhibition model:

$$(2) v = \frac{v_{max}[S]}{K_m + [S] \left(1 + \frac{[S]}{K_{si}}\right)}$$

Where K_{si} is the constant describing the substrate inhibition interaction. This model is based on mechanism in which a second molecule of substrate binds to preformed enzyme-substrate complex ($E \cdot S$) and thus acts as uncompetitive inhibitor of the reaction.

For the calculation of enzyme inhibition constants, the obtained data were fitted to the models for **competitive** (eq. 3), **mixed-type** (eq. 4), **noncompetitive** (eq. 5), and **uncompetitive inhibition** (eq. 6) (Copeland, 2005):

$$(3) v = \frac{V_{max}[S]}{[S] + K_m \left(1 + \frac{[I]}{K_{ic}}\right)}$$

$$(4) v = \frac{V_{max}[S]}{[S] \left(1 + \frac{[I]}{\alpha K_{im}}\right) + K_m \left(1 + \frac{[I]}{K_{im}}\right)}$$

$$(5) v = \frac{V_{max}[S]}{([S] + K_m) \left(1 + \frac{[I]}{K_{in}}\right)}$$

$$(6) v = \frac{V_{max}[S]}{[S] \left(1 + \frac{[I]}{\alpha K_{iu}}\right) + K_m}$$

Where K_{ic} , K_{im} , K_{in} , and K_{iu} are the competitive, mixed-type, noncompetitive, and uncompetitive inhibition constants, respectively. The coefficient α in eqs. 4 and 6 represents the relative difference in inhibitor's binding affinity between the free enzyme (competitive modality) and the E•S complex (uncompetitive modality).

The reversible transfer of glucuronic acid from UDPGA to the aglycone substrate is described in this study by the general reaction: $AX + B \rightleftharpoons BX + A$, in which AX, B, BX, and A represent UDPGA, the aglycone substrate, the glucuronide conjugate and UDP, respectively. For the analysis of bisubstrate enzyme kinetic data, the initial velocities were fitted to the following equations:

Compulsory-order ternary-complex model based on a steady-state assumption (Cornish-Bowden, 2012):

$$(7) v = \frac{V_{max}[AX][B]}{K_{iAX}K_{mB} + K_{mB}[AX] + K_{mAX}[B] + [AX][B]}$$

Where $[AX]$ and $[B]$ are the concentrations of UDPGA and aglycone substrate, respectively, V_{max} is the limiting velocity at saturating concentration of both AX and B, K_{iAX} is the equilibrium dissociation constant for the $E + AX \rightleftharpoons E \cdot AX$ reaction, K_{mAX} is the limiting Michaelis constant for AX when B is saturating, and K_{mB} is the limiting Michaelis constant for B when AX is saturating. This model assumes that substrate AX binds first and B is the second-binding substrate. In the case of the reverse reaction, UDP (A) and 4-MUG (BX) are considered as the first and second substrates, respectively (Fig. 8). The Haldane relationship for the compulsory-order ternary-complex mechanism is given by $K_{eq} = V_{max}^f K_{mBX} K_{iA} / V_{max}^r K_{mB} K_{iAX}$, where V_{max}^f and V_{max}^r are the limiting velocities in the forward and reverse direction, respectively.

Compulsory-order ternary-complex model based on a steady-state assumption with substrate inhibition (Cornish-Bowden, 2012):

$$(8) v = \frac{v_{max}[A][B]}{K_{iAX}K_{mB} + K_{mB}[AX] + K_{mAX}[B] + [AX][B]\left(1 + \frac{[B]}{K_{siB}}\right)}$$

Where K_{siB} is a constant that describes the substrate inhibition interaction. This model assumes that AX and B are first and second enzyme substrates, respectively, and that substrate inhibition arises from binding of the second substrate, B, to the “wrong” binary complex, $E \cdot A$, instead of $E \cdot AX$ (see Fig. 8).

Compulsory-order ternary-complex model based on a rapid-equilibrium assumption (Alberty, 2011, Copeland, 2000):

$$(9) v = \frac{v_{max}[AX][B]}{K_{sAX}K_{sB} + K_{sB}[AX] + [AX][B]}$$

Where $K_{s_{AX}}$ is the equilibrium dissociation constant for the E•AX complex ($E + AX \rightleftharpoons E \cdot AX$) and K_{s_B} is the equilibrium dissociation constant for the E•AX•B complex ($E \cdot AX + B \rightleftharpoons E \cdot AX \cdot B$). This model assumes that AX and B are the first and second binding substrates, respectively.

Random-order ternary-complex model based on a rapid-equilibrium assumption
(Alberty, 2011):

$$(10) v = \frac{v_{max}[AX][B]K_{iB}}{K_B K_{i_{AX}}[B] + K_{iB}[AX][B] + K_B K_{i_{AX}}[AX] + K_B K_{i_{AX}} K_{iB}}$$

Where $K_{i_{AX}}$ and K_{iB} are the equilibrium dissociation constants for the E•AX and E•B complexes, respectively. K_B is the first equilibrium dissociation constant for the E•AX•B complex ($E \cdot AX \cdot B \rightleftharpoons E \cdot AX + B$). K_A , the second equilibrium dissociation constant for the E•AX•B complex ($E \cdot AX \cdot B \rightleftharpoons E \cdot B + AX$), is not included in this equation but can be calculated from the following relationship: $K_{iA} K_B = K_{iB} K_A$.

Substituted-enzyme (ping-pong bi-bi) model based on a steady-state assumption

(Cornish-Bowden, 2012):

$$(11) v = \frac{v_{max}[AX][B]}{K_{m_{AX}}[B] + K_{m_B}[AX] + [AX][B]}$$

Where $K_{m_{AX}}$ and K_{m_B} are the limiting Michaelis constants for AX and B, as in eq. 7. This model also implicitly assumes mechanistically reasonable compulsory-order mechanism, where AX and B are the first and second binding substrates, respectively.

Substituted-enzyme (ping-pong bi-bi) model based on a steady-state assumption with substrate inhibition (Cornish-Bowden, 2012):

$$(12) v = \frac{v_{max}[AX][B]}{K_{m_{AX}}[B] \left(1 + \frac{[B]}{K_{siB}}\right) + K_{m_B}[AX] + [AX][B]}$$

DMD #47746

In this model substrate inhibition arises from B binding to the free enzyme ($E + B \rightleftharpoons E \cdot B$) and K_{siB} represents the dissociation constant for the $E \cdot B$ complex.

Results

Substrates binding to BSA and insect cell membranes. The binding of entacapone, 4-MU, and 1-naphthol to BSA, both 0.1% and 1%, and to insect cell membranes, the "Bac control" membranes that lack any human UGT, was measured in this study by the RED system. The results of the binding assays with this system, in the way we performed them (see *Materials and Methods* for technical details) were in good agreement with the binding results for entacapone and 4-MU that we previously obtained using ultrafiltration (Manevski et al., 2011) (Fig. 1). For all the tested compounds in this study, the equilibrium was reached within 8 h of incubation in the RED device, under constant shaking. Overnight incubation seemed more susceptible to inaccuracies due to volume shifts, caused by hydrostatic pressure, and increased risk of compounds instability (results not shown). The nonspecific binding to the RED device of the tested compounds was low ($\leq 20\%$).

Entacapone binds strongly to 0.1% BSA and, as previously reported (Manevski et al., 2011), the measured f_u for this drug exhibits hyperbolic saturable binding profile (Fig. 1A). The 4-MU binding to 0.1 and 1% BSA was partially concentration dependent (Fig. 1B), as previously found using the ultrafiltration method (Manevski et al., 2011). The binding of 1-naphthol to 0.1% BSA was rather low and concentration independent, $f_u = 0.78 \pm 0.01$ (average \pm S.E.; Fig. 1C).

The results of the binding experiments of entacapone, 4-MU, and 1-naphthol to insect cells membranes revealed that in the presence of up to 0.2 mg/mL (total protein), the highest protein concentration used in this work, the binding of all the tested compounds was low. The binding of UDPGA, UDP, and 4-MUG to 0.1% BSA was negligible (data not shown).

BSA effects on the enzyme kinetics of 1-naphthol glucuronidation by UGT1A9. We have examined 1-naphthol glucuronidation by UGT1A9 since, for the purpose of this study, it is a

high affinity but low turnover substrate that can serve as an inhibitor for the aglycone substrate binding (Luukkanen et al., 2005). The question we tried to answer in this experiment was whether or not the (low rate) glucuronidation of 1-naphthol by UGT1A9, as well as the usefulness of this compound as inhibitor for UGT1A9, are affected by the presence of BSA in the reaction medium. The addition of 0.1% BSA affected the enzyme kinetics of 1-naphthol glucuronidation by UGT1A9 in a similar manner to its effect on the glucuronidation of entacapone and 4-MU by UGT1A9, namely K_m decrease and V_{max} increase (Manevski et al., 2011). It lowered the K_m of UGT1A9 in the 1-naphthol glucuronidation reaction from 376 ± 36 (CI 95%, 302–449) to 177 ± 14 nM (CI 95%, 149–206) and increased the reaction's V_{max} from 0.042 ± 0.002 (CI 95%, 0.037–0.048) to 0.068 ± 0.002 (CI 95%, 0.064–0.073) $\text{nmol}\cdot\text{min}^{-1}\cdot\text{mg}^{-1}$ (Fig. 2). The results are presented as the average \pm S.E., and the calculated 95% CI are given in parenthesis. Although some deviation from the hyperbolic kinetics was observed at low concentrations of 1-naphthol, presumably due to technical difficulties in measuring very low glucuronidation rates, the reaction's kinetics was, generally, well described by the Michaelis-Menten model ($r^2 \geq 0.98$).

Bisubstrate kinetics of 4-MU glucuronidation by UGT1A9. With the aim of understanding the enzyme kinetics mechanism of UGT-catalyzed reactions and how it is affected by the inclusion of BSA, we studied the bisubstrate kinetics of 4-MU glucuronidation by UGT1A9. The results of this analysis, from the perspective of both substrates, are presented as initial velocity vs. substrate concentration and as Eadie-Hofstee plots (Fig. 3). The data points were fitted to eqs. 7–12 (see *Materials and Methods*) and the best model was selected based on curve fitting parameters (see *Materials and Methods*), experimental evidence, and theoretical considerations (Table 3).

The bisubstrate enzyme kinetics assays, in the absence (as previously done) and in the presence of BSA, were initially carried out using a lower concentration range of 4-MU, where substrate inhibition is not clearly apparent to the eye (Fig. 3A and 3B). The primary Eadie-Hofstee transforms of the data, from the perspective of both substrates, indicated a common intersection point in the second quadrant, left of the y-axis – a pattern characteristic of ternary-complex mechanism. Despite many efforts, however, we did not obtain a well-defined intersection points in Figs. 3A and 3B. Nevertheless, considering the clearly different intersection point from the one expected in the case of substituted-enzyme mechanism (on the x-axis in the first quadrant), we think that our results clearly support the formation of a ternary-complex. The formation of ternary-complex was also supported by the poor fit of the substituted-enzyme equation (eq. 11) to the experimental data points. On the other hand, the data (Figs. 3A and 3B) fitted well to the equations for compulsory-order ternary-complex model based on the steady-state assumption (eq. 7), as well as to the random-order ternary-complex model based on the rapid-equilibrium assumption (eq. 10). The fit to the compulsory-order ternary-complex model, based on the rapid-equilibrium assumption (eq. 9), was not as good, however. The compulsory-order models were also supported by the product and dead-end inhibition studies (see text below, Figs. 6 and 7, Table 4). The inclusion of BSA did not qualitatively change the bisubstrate kinetics of 4-MU glucuronidation, even if it significantly affected the magnitude of the enzyme kinetic parameters (Table 3). Analysis of the bisubstrate kinetic data with eq. 7 indicates that the inclusion of BSA led to an increase of both the apparent 4-MU affinity (lower K_m value) and the reaction limiting velocity (higher V_{max}). The apparent affinity for UDPGA, however, was lower (higher K_m value) in the presence of BSA.

The second set of bisubstrate kinetics reactions was carried out using higher concentrations of 4-MU, in the presence of BSA (Fig. 4). Substrate inhibition became apparent at 4-MU concentrations higher than 40 μM and, interestingly, was also potentiated by higher

concentrations of UDPGA. The data fitted well to the steady-state compulsory-order ternary-complex model with substrate inhibition (eq. 8, Table 3), yielding a K_{si} value for 4-MU of approx. 50-fold higher than the corresponding K_m value. As in the case of bisubstrate kinetics at lower concentrations of 4-MU (Fig. 3), the lines in the Eadie-Hofstee plots of the bisubstrate kinetics with substrate inhibition showed a common intersection point in the second quadrant (Figs. 4A and 4B), the pattern indicative of ternary-complex formation. It should be noted, however, that the intersection pattern appears different from the perspective of UDPGA at very high concentrations of 4-MU (Fig. 4B, lines marked with dotted line), in the region where substrate inhibition becomes pronounced. This result suggests that potential substrate inhibition by the aglycone substrate should always be taken into account when enzyme kinetics of UDPGA is studied. Otherwise, erroneous conclusions about the enzyme kinetic parameters may be reached.

In order to understand the overall enzyme kinetic mechanism, we have also investigated the reverse reaction, an approach that was rarely taken in previous UGT studies, particularly since recombinant UGTs became available and ensure that the analysis is conducted on a single enzyme rather than a mixture of different UGTs (Vessey and Zakim, 1972, Rao et al., 1976, Matern et al., 1991). Hence, the bisubstrate enzyme kinetics, in the presence of BSA, was also studied for the reverse reaction, namely the formation of 4-MU and UDPGA from 4-MUG and UDP (Fig. 5). Special attention was paid to the prevention of possible non-enzymatic 4-MUG hydrolysis and to exclude the possibility that other enzymes in the insect cell membrane are catalyzing UDPGA formation from 4-MUG and UDP. The latter was examined using the “Bac-control membranes” that lacked any recombinant UGT and the assays revealed no significant 4-MU or UDPGA formation upon addition of 4-MUG and UDP. The reverse reaction, in the presence of BSA, was rather fast under optimal conditions, namely in the presence of high concentrations of 4-MUG (Fig. 5, Table 3). The results of the bisubstrate

reverse reaction indicated that it follows a ternary-complex mechanism, as can be seen from the common intersection point in the second quadrant of the Eadie-Hofstee plots, just left of the y-axis. It may be noted here that the data points from the reverse reaction are slightly biphasic and, therefore, may indicate a more complex enzyme kinetic model than currently applied (eq. 7). Nevertheless, in the current study it was important for us to estimate the enzyme kinetic parameters of the reverse reaction in the context of the overall enzyme kinetic mechanism. From this point of view, the equation of compulsory-order ternary-complex reaction mechanism serves as a good approximation, even if we cannot exclude at this stage a more complex behavior. Future studies may address this issue in more detail. The K_m value for 4-MUG was approximately 500-fold higher than the K_m value for 4-MU, whereas the K_m value for UDP was approximately one order of magnitude lower than the corresponding value for UDPGA. Based on the Haldane relationship for the compulsory-order ternary-complex mechanism (see *Materials and Methods*), the thermodynamic equilibrium constant of the reaction in the presence of BSA is $K_{eq} = 574$.

One can expect unique relationships between the enzyme kinetic parameters and the individual rate constants in the compulsory-order ternary-complex mechanism (Cornish-Bowden, 2012). Unfortunately, due to lack of purified and fully active UGT1A9 enzyme, we could only determine the relative ratio of the rate constants, not the absolute values. For comparison, the results were normalized by arbitrarily setting the value of V_{max}^f , the limiting reaction velocity in the forward direction, to 1 and then using the expression $V_{max}^f = k_{cat}^f [E]$, where $[E]$ is the molar concentration of the enzyme (Table 5). It is worth noting here that although the first-order and second-order rate constants cannot be directly compared, a pseudo-first-order rate constant such as $k_1[AX]$ can be compared with other first-order constants. These results indicate that the catalytic rate constant in the forward direction, k_{cat}^f , is about 11-fold higher than the corresponding catalytic rate constant in the reverse reaction k_{cat}^r .

Inhibition studies of UGT1A9-catalyzed 4-MU glucuronidation in the presence of 0.1% BSA. The bisubstrate enzyme kinetic experiments confirmed the existence of ternary-complex. In order to distinguish between compulsory-order and random-order mechanism, we performed product inhibition studies with UDP and dead-end inhibition studies with 1-naphthol. As noted above, 1-naphthol is a high affinity but low turnover substrate for UGT1A9 ($K_m = 177 \pm 14$ nM; $V_{max} = 0.068 \pm 0.002$ nmol·min⁻¹·mg⁻¹) and, under specific experimental conditions, can be regarded as a 4-MU-competing dead-end inhibitor of UGT1A9.

The results revealed that UDP is a mixed-type and competitive inhibitor of 4-MU glucuronidation with respect to 4-MU and UDPGA, respectively (Figs. 6A and 7A, Table 4). On the other hand, 1-naphthol was found to be a mixed-type inhibitor with respect to 4-MU (Fig. 6B, Table 4), although with the competitive component of the inhibition clearly prevailing ($\alpha = 7.38 \pm 1.75$; average \pm S.E.; Table 4). Importantly, however, 1-naphthol was uncompetitive inhibitor with respect to UDPGA (Fig. 7B, Table 4). In addition, it may be added that the determined values of 1-naphthol's K_m (177 ± 14 nM) and mixed-type K_i with respect to 4-MU (19.8 ± 2.7 nM) are not in good agreement with each other. The observed discrepancy may be due, at least partially, to the different physical meaning of the K_m and K_i values. While the K_i is a true equilibrium-dissociation constant of the enzyme•1-naphthol complex (or in the case of compulsory-order substrate binding, the enzyme•UDPGA•1-naphthol complex), the K_m is a pseudo-affinity constant that may or may not equal the true substrate dissociation constant.

Discussion

We recently found that the “albumin effect” in human UGT1A9 is different than in UGT2B7, since it both decreases the K_m and increases the V_{max} in the 4-MU and UGT1A9-catalyzed entacapone glucuronidation reactions (Manevski et al., 2011). This finding prompted us to reexamine the reaction mechanism of UGT1A9 and whether or not it is affected by the presence of BSA. We selected 4-MU as an aglycone substrate for the detailed enzyme kinetic analysis since it is a high affinity–high turnover substrate and exhibits substrate inhibition at high concentrations, a feature typical for many UGT-catalyzed reactions. In addition, 4-MU and 4-MUG are commercially available and, importantly, are highly fluorescent, making them suitable for sensitive detection.

For accurate analysis of the BSA effect it is essential to determine the free drug concentration in the presence of the used BSA concentration. For such measurements we have now used the RED method (Waters et al., 2008) and compared the results with our previous data that were obtained using ultrafiltration (Manevski et al., 2011). The two methods provide very similar results for both entacapone and 4-MU binding to BSA, when taking into account the non-specific drug binding to the device (Fig. 1). The inclusion of $MgCl_2$, UDPGA, or UDP did not significantly alter the substrates binding to BSA. In contrast, the addition of membrane samples (0.02–0.2 mg/mL) significantly modulated the entacapone binding to 0.1% BSA and should be taken into account (Manevski et al., 2011).

To examine whether or not BSA affects the reaction mechanism of UGT1A9 we have used bisubstrate kinetic analysis of 4-MU glucuronidation by UGT1A9. The results, both in the forward and the reverse directions, strongly suggested that the 4-MU glucuronidation reaction proceeds through the formation of ternary-complex, regardless of whether or not BSA was added to the assay (Figs. 3, 4, and 5; Table 3). The bisubstrate kinetic data were best described

by a steady-state compulsory-order ternary-complex model, even though evidence from complementary inhibition experiments may be needed to fully prove this (see below). BSA presence affected the forward reaction by lowering the K_m value for 4-MU and increasing the V_{max} value. In addition, and somewhat surprisingly, it increased the K_m value of UGT1A9 for UDPGA (Fig. 3, Table 3). The inclusion of BSA, however, did not qualitatively affect the bisubstrate kinetics model (Fig 3, see Eadie-Hofstee insets).

The analysis of bisubstrate kinetics results in the forward and reverse directions, when both were assayed in the presence of BSA, revealed that UGT1A9 has about 500-fold higher affinity for 4-MU than for 4-MUG (Table 3). Interestingly, the apparent affinity of the enzyme for UDP, as measured in the reverse reaction, is an order of magnitude higher than for UDPGA in the forward reaction (Table 3). Taken together, the results suggest that the reverse reaction is mainly limited by the poor affinity of the enzyme for 4-MUG. Another factor that contributes to making the reaction proceed almost exclusively in the forward direction in the human cell is that the k_{-2} (first-order rate constant for $E \cdot AX \cdot B \rightarrow E \cdot AX + B$ reaction) is much smaller than k_3 (first-order rate constant for $E \cdot AX \cdot B \rightarrow E \cdot A + BX$ reaction) (Fig. 8 and Table 5). A comparison of the relative individual rate constants also shows that the first-order rate constants in the forward direction, such as k_3 and k_4 , are within the same order of magnitude as k_{-1} , an observation that supports the steady-state assumption (Fig. 8, Table 5). Based on the measured enzyme kinetic parameters and the Haldane relationship, the equilibrium constant of the overall reaction is large, $K_{eq} = 574$. Nevertheless, as we clearly show in this study (Fig. 5), the reverse reaction can also be performed and analyzed under, more-or-less, conditions of standard *in vitro* UGTs assays.

The presence of substrate inhibition at high concentrations of 4-MU (Fig. 4), that appears to be stimulated by the presence of high UDPGA concentrations, provides evidence for a steady-

state compulsory-order ternary-complex reaction mechanism (see also Luukkanen et al., 2005). In this mechanism, either the second substrate or the first product of the reaction may bind to a "wrong" binary complex. The results of the bisubstrate kinetic analyses support the assumption that in the case of the studied reaction, UDPGA and 4-MU are the first and second binding substrates, respectively, and that substrate inhibition probably occurs due to 4-MU binding to a "wrong" binary complex, E•UDP, rather than to the "correct" binary complex, E•UDPGA (Fig. 8). The measured relatively high affinity of UDP to the free enzyme may explain why substrate inhibition is commonly observed in UGT-catalyzed reactions, especially if the initial rate conditions are not strictly followed and the UDP concentration increases due to its accumulation during the forward reaction (Table 3). This should raise awareness about potential problems in substrate depletion experiments with the UGTs. In such experiments, contrary to initial-rate assays, the accumulation of UDP is likely to slow down the aglycone substrate depletion.

Substrate inhibition can also occur in the random-order ternary-complex mechanism, where 4-MU may also bind to E•UDP complex. However, if the rapid-equilibrium assumption is valid, the E•UDP complex concentration is zero in the absence of accumulated or added products. Since 4-MU cannot bind to enzyme species that are not present, the rapid-equilibrium random-order ternary-complex mechanism can be excluded based on this observation. However, the non-rapid-equilibrium random-order ternary-complex mechanism may not be ruled out based on bisubstrate kinetics only. The rapid-equilibrium compulsory-order ternary-complex, however, may be excluded based on herein measured and reported rate constant magnitudes (Table 5; Luukkanen et al., 2005), substrate inhibition, and poor fit to experimental data.

UDP was found to be a competitive inhibitor with respect to UDPGA, and mixed-type inhibitor with respect to 4-MU (Figs. 6A and 7A, Table 4). Such inhibition patterns agree well

with the previously published data (Luukkanen et al., 2005, Fujiwara et al., 2008) and are possible for both random-order and compulsory-order ternary-complex mechanisms. However, if the reaction follows the compulsory-order ternary-complex mechanism, as indicated by the bisubstrate kinetic analyses and substrate inhibition, the UDP inhibition results support the suggestion that UDPGA is the first binding substrate in a compulsory-order mechanism.

In line with previous finding in the absence of BSA (Luukkanen et al., 2005), 1-naphthol is a predominantly competitive inhibitor of UGT1A9 with respect to 4-MU ($\alpha = 7.38 \pm 1.75$) but, importantly, uncompetitive with respect to UDPGA (Figs. 6B and 7B, Table 4). This result indicates that 1-naphthol, an inhibitor that probably competes with 4-MU for the aglycone substrate-binding site, does not compete for the same enzyme species as UDPGA. The uncompetitive inhibition pattern arises from 1-naphthol binding to the pre-formed E•UDPGA complex, rather than to the free enzyme. This uncompetitive inhibition provides strong evidence that UGT substrates are binding in a compulsory fashion in which the initial binding of UDPGA increases the affinity for the aglycone substrate. Such an affinity increase could be a result of a conformational change in the enzyme upon UDPGA binding, the involvement of the bound UDPGA molecule itself in the binding of the aglycone substrate (see Fig. 9 of Itäaho et al., 2010), or both. We can also expect that the reverse reaction should be structurally analogous to the forward reaction, and that the second product of the forward reaction (UDP) should be the structural analogue of the first substrate (UDPGA).

Based on the available evidence, UGT1A9 follows a steady-state compulsory-order ternary-complex mechanism, regardless of whether or not BSA is present (Fig. 8). One may then ask how BSA interferes with this reaction mechanism to affect the apparent substrate affinities and the reaction V_{\max} . Taking into account that the presence of BSA increases the apparent affinity for 4-MU and decreases the apparent affinity for UDPGA, it may be proposed that BSA

removes internal inhibitors that are competitive and/or noncompetitive with respect to the aglycone substrate, but are uncompetitive with respect to UDPGA. The uncompetitiveness of the BSA-removed inhibitors with respect to UDPGA would explain why the affinity for this cosubstrate apparently decreases in the presence of BSA. Such inhibitors, tentatively marked as I_1 and I_2 in the reaction scheme (Fig. 8) would not (or poorly) bind to the free enzyme, but would bind with higher affinity to the binary E•UDPGA complex or the ternary E•UDPGA•4-MU complex.

If the UGT1A9 inhibitor(s) source is the membrane in which the enzyme is located, it may be suggested that the differences in lipid composition between the insect cell membranes (see Marheineke et al., 1998, for the lipid composition of *Sf9* membranes) to the human liver membranes could lead to differences in the BSA effects between the recombinant UGT and the native enzyme. Presently, we cannot discard this possibility, particularly regarding the magnitude of the BSA effect when different substrates are used. Nevertheless, recent studies on the BSA effects demonstrated only minor influences of the membrane source on the BSA effects in UGT1A9 (Manevski et al., 2011; Shiraga et al., 2012), or UGTs 1A1, 1A4, 1A6, and 2B7 (Walsky et al., 2012). Hence, the currently available results do not indicate significant differences between *Sf9* membranes and HLM as sources of the inhibitory fatty acids that are removed by BSA, when present during the glucuronidation reaction. While the exact nature and number of these inhibitors is currently unknown, the improved understanding of the UGT reaction mechanism and the BSA effects may help to rationalize and predict the BSA effect in future.

Acknowledgements

We would like to thank Johanna Mosorin for skilful technical assistance.

Author contributions:

Participated in research design: N.M., M.F.

Conducted experiments: N.M.

Contributed new reagents or analytical tools:

Performed data analysis: N.M.

Wrote or contributed to the writing of the manuscript: N.M., J.Y-K., M.F.

References

- Alberty RA. (2011) *Enzyme Kinetics: Rapid-Equilibrium Applications of Mathematica*, First Edition ed. John Wiley & Sons, Inc., Hoboken, NJ, USA.
- Axelrod J, Inscoe JK, and Tomkins GM. (1958) Enzymatic synthesis of N-glucosyluronic acid conjugates. *J Biol Chem* **232**:835-841.
- Bernard O and Guillemette C. (2004) The main role of UGT1A9 in the hepatic metabolism of mycophenolic acid and the effects of naturally occurring variants. *Drug Metab Dispos* **32**:775-778.
- Bock KW. (2010) Functions and transcriptional regulation of adult human hepatic UDP-glucuronosyl-transferases (UGTs): mechanisms responsible for interindividual variation of UGT levels. *Biochem Pharmacol* **80**:771-777.
- Copeland RA. (2000) *Enzymes: A Practical Introduction to Structure, Mechanism, and Data Analysis*, Second edition ed. John Wiley & Sons, Inc., New York, NY, USA.
- Copeland RA. (2005) *Evaluation of Enzyme Inhibitors in Drug Discovery*, First Edition ed. John Wiley & Sons, Inc., Hoboken, NJ, USA.
- Cornish-Bowden A. (2012) *Fundamentals of Enzyme Kinetics*, 4th ed. Wiley-Blackwell, Weinheim, Germany.
- Court MH, Zhang X, Ding X, Yee KK, Hesse LM, and Finel M. (2012) Quantitative distribution of mRNAs encoding the 19 human UDP-glucuronosyltransferase enzymes in 26 adult and 3 fetal tissues. *Xenobiotica* **42**:266-277.
- Dowd J and Riggs D. (1965) A Comparison of Estimates of Michaelis-Menten Kinetic Constants from various Linear Transformations. *J Biol Chem* **240**:863-&.
- Falany CN, Green MD, and Tephly TR. (1987) The enzymatic mechanism of glucuronidation catalyzed by two purified rat liver steroid UDP-glucuronosyltransferases. *J Biol Chem* **262**:1218-1222.
- Fujiwara R, Nakajima M, Yamanaka H, Katoh M, and Yokoi T. (2008) Product inhibition of UDP-glucuronosyltransferase (UGT) enzymes by UDP obfuscates the inhibitory effects of UGT substrates. *Drug Metab Dispos* **36**:361-367.
- Itaaho K, Laakkonen L, and Finel M. (2010) How many and which amino acids are responsible for the large activity differences between the highly homologous UDP-glucuronosyltransferases (UGT) 1A9 and UGT1A10? *Drug Metab Dispos* **38**:687-696.
- Jemnitz K, Heredi-Szabo K, Janossy J, Ioja E, Vereczkey L, and Krajcsi P. (2010) ABC2/Abcc2: a multispecific transporter with dominant excretory functions. *Drug Metab Rev* **42**:402-436.
- Johnson LP and Fenselau C. (1978) Enzymatic conjugation and hydrolysis of [¹⁸O]isoborneol glucuronide. *Drug Metab Dispos* **6**:677-679.

Kaivosaaari S, Toivonen P, Aitio O, Sipila J, Koskinen M, Salonen JS, and Finel M. (2008) Regio- and stereospecific N-glucuronidation of medetomidine: the differences between UDP glucuronosyltransferase (UGT) 1A4 and UGT2B10 account for the complex kinetics of human liver microsomes. *Drug Metab Dispos* **36**:1529-1537.

Koster AS and Noordhoek J. (1983) Kinetic properties of the rat intestinal microsomal 1-naphthol:UDP-glucuronosyl transferase. Inhibition by UDP and UDP-N-acetylglucosamine. *Biochim Biophys Acta* **761**:76-85.

Kurkela M, Patana AS, Mackenzie PI, Court MH, Tate CG, Hirvonen J, Goldman A, and Finel M. (2007) Interactions with other human UDP-glucuronosyltransferases attenuate the consequences of the Y485D mutation on the activity and substrate affinity of UGT1A6. *Pharmacogenet Genomics* **17**:115-126.

Kurkela M, Garcia-Horsman JA, Luukkanen L, Morsky S, Taskinen J, Baumann M, Kostiaainen R, Hirvonen J, and Finel M. (2003) Expression and characterization of recombinant human UDP-glucuronosyltransferases (UGTs). UGT1A9 is more resistant to detergent inhibition than other UGTs and was purified as an active dimeric enzyme. *J Biol Chem* **278**:3536-3544.

Lautala P, Ethell BT, Taskinen J, and Burchell B. (2000) The specificity of glucuronidation of entacapone and tolcapone by recombinant human UDP-glucuronosyltransferases. *Drug Metab Dispos* **28**:1385-1389.

Luukkanen L, Taskinen J, Kurkela M, Kostiaainen R, Hirvonen J, and Finel M. (2005) Kinetic characterization of the 1A subfamily of recombinant human UDP-glucuronosyltransferases. *Drug Metab Dispos* **33**:1017-1026.

Mackenzie PI, Bock KW, Burchell B, Guillemette C, Ikushiro S, Iyanagi T, Miners JO, Owens IS, and Nebert DW. (2005) Nomenclature update for the mammalian UDP glycosyltransferase (UGT) gene superfamily. *Pharmacogenet Genomics* **15**:677-685.

Manevski N, Moreolo PS, Yli-Kauhaluoma J, and Finel M. (2011) Bovine serum albumin decreases Km values of human UDP-glucuronosyltransferases 1A9 and 2B7 and increases Vmax values of UGT1A9. *Drug Metab Dispos* **39**:2117-2129.

Marheineke K, Grunewald S, Christie W, and Reilander H. (1998) Lipid composition of *Spodoptera frugiperda* (Sf9) and *Trichoplusia ni* (Tn) insect cells used for baculovirus infection. *FEBS Lett* **441**:49-52.

Matern H, Lappas N, and Matern S. (1991) Isolation and characterization of hyodeoxycholic acid: UDP-glucuronosyltransferase from human liver. *Eur J Biochem* **200**:393-400.

Matern H, Matern S, and Gerok W. (1982) Isolation and characterization of rat liver microsomal UDP-glucuronosyltransferase activity toward chenodeoxycholic acid and testosterone as a single form of enzyme. *J Biol Chem* **257**:7422-7429.

Miners JO, Mackenzie PI, and Knights KM. (2010) The prediction of drug-glucuronidation parameters in humans: UDP-glucuronosyltransferase enzyme-selective substrate and inhibitor

probes for reaction phenotyping and in vitro-in vivo extrapolation of drug clearance and drug-drug interaction potential. *Drug Metab Rev* **42**:189-201.

Ohno S and Nakajin S. (2009) Determination of mRNA expression of human UDP-glucuronosyltransferases and application for localization in various human tissues by real-time reverse transcriptase-polymerase chain reaction. *Drug Metab Dispos* **37**:32-40.

Patana AS, Kurkela M, Goldman A, and Finel M. (2007) The human UDP-glucuronosyltransferase: identification of key residues within the nucleotide-sugar binding site. *Mol Pharmacol* **72**:604-611.

Potrepka RF and Spratt JL. (1972) A study on the enzymatic mechanism of guinea-pig hepatic-microsomal bilirubin glucuronyl transferase. *Eur J Biochem* **29**:433-439.

Rao ML, Rao GS, and Breuer H. (1976) Investigations on the kinetic properties of estrone glucuronyltransferase from pig kidney. *Biochim Biophys Acta* **452**:89-100.

Rowland A, Knights KM, Mackenzie PI, and Miners JO. (2008) The "albumin effect" and drug glucuronidation: bovine serum albumin and fatty acid-free human serum albumin enhance the glucuronidation of UDP-glucuronosyltransferase (UGT) 1A9 substrates but not UGT1A1 and UGT1A6 activities. *Drug Metab Dispos* **36**:1056-1062.

Rowland A, Gaganis P, Elliot DJ, Mackenzie PI, Knights KM, and Miners JO. (2007) Binding of inhibitory fatty acids is responsible for the enhancement of UDP-glucuronosyltransferase 2B7 activity by albumin: implications for in vitro-in vivo extrapolation. *J Pharmacol Exp Ther* **321**:137-147.

Sanchez E and Tephly TR. (1975) Morphine metabolism. IV. Studies on the mechanism of morphine: uridine diphosphoglucuronyltransferase and its activation by bilirubin. *Mol Pharmacol* **11**:613-620.

Shiraga T, Yajima K, Suzuki K, Suzuki K, Hashimoto T, Iwatsubo T, Miyashita A, and Usui T. (2012) Identification of UDP-Glucuronosyltransferases Responsible for the Glucuronidation of Darexaban, an Oral Factor Xa Inhibitor, in Human Liver and Intestine. *Drug Metab Disposition* **40**:276-282.

Soars MG, Petullo DM, Eckstein JA, Kasper SC, and Wrighton SA. (2004) An assessment of udp-glucuronosyltransferase induction using primary human hepatocytes. *Drug Metab Dispos* **32**:140-148.

Vessey DA and Zakim D. (1972) Regulation of microsomal enzymes by phospholipids. V. Kinetic studies of hepatic uridine diphosphate-glucuronyltransferase. *J Biol Chem* **247**:3023-3028.

Walsky RL, Bauman JN, Bourcier K, Giddens G, Lapham K, Negahban A, Ryder TF, Obach RS, Hyland R, and Goosen TC. (2012) Optimized Assays for Human UDP-Glucuronosyltransferase (UGT) Activities: Altered Alamethicin Concentration and Utility to Screen for UGT Inhibitors. *Drug Metab Dispos* **40**:1051-1065.

Waters NJ, Jones R, Williams G, and Sohal B. (2008) Validation of a rapid equilibrium dialysis approach for the measurement of plasma protein binding. *J Pharm Sci* **97**:4586-4595.

Yin H, Bennett G, and Jones JP. (1994) Mechanistic studies of uridine diphosphate glucuronosyltransferase. *Chem Biol Interact* **90**:47-58.

Zhang H, Tolonen A, Rousu T, Hirvonen J, and Finel M. (2011) Effects of cell differentiation and assay conditions on the UDP-glucuronosyltransferase activity in Caco-2 cells. *Drug Metab Dispos* **39**:456-464.

Footnotes

This study was financially supported by the Sigrid Juselius Foundation, Finland; the Finnish Graduate School in Pharmaceutical Research; the University of Helsinki Research Foundation grant for young researchers; the Academy of Finland [grant number 120975].

Legends for figures

Figure 1. Binding of entacapone (A), 4-MU (B), and 1-naphthol (C) to BSA. The points represent the average of two samples (variation between two replicates was less than 15%). The results from the RED system and from ultrafiltration are presented by solid and dashed lines, respectively. In the case of entacapone (A), the correlation between the results from the two methods is presented in the inset.

Figure 2. Enzyme kinetics of 1-naphthol glucuronidation by UGT1A9 without BSA (●, dashed line) and in the presence of 0.1% BSA (■, solid line). The points represent an average of three samples \pm S.E. Glucuronidation rates are presented as measured initial rates in $\text{nmol}\cdot\text{min}^{-1}\cdot\text{mg}^{-1}$ of UGT1A9-enriched insect cell membranes. The results are presented as the average \pm S.E., and the calculated 95% CI are given in the parenthesis. The Eadie-Hofstee transform of the data are presented as inset.

Figure 3. Bisubstrate enzyme kinetics of UGT1A9-catalyzed 4-MU glucuronidation and the BSA effects on it. The results in the absence of BSA are shown in the upper panels (A) and results from assays in the presence of 0.1% BSA in the lower panels (B). The points represent the average of two samples (variation between two replicates was less than 15%). Glucuronidation rates are presented as measured initial rates in $\text{nmol}\cdot\text{min}^{-1}\cdot\text{mg}^{-1}$ of UGT1A9-enriched insect cell membranes. The derived kinetic constants are presented in Table 3. The Eadie-Hofstee transforms of the data, both from the perspectives of 4-MU (A1 and B1) and of UDPGA (A2 and B2), are presented in the panels on the right.

Figure 4. The BSA effects on the bisubstrate enzyme kinetics of 4-MU glucuronidation by UGT1A9, at higher concentrations of 4-MU. For further details see legend to Fig. 3. The Eadie-Hofstee transforms of the data, both from the perspectives of 4-MU (A) and of UDPGA (B), are presented in the panels on the right. The lines in the Eadie-Hofstee plot 4B at very

high concentrations of 4-MU, the region where aglycone substrate inhibition becomes pronounced, are indicated by dashed lines.

Figure 5. Bisubstrate enzyme kinetics of the UGT1A9-catalyzed reverse reaction, glucuronic acid transfer from 4-MUG to UDP. The reactions were carried out in the presence of 0.1% BSA and the points represent the average of two samples (variation between two replicates was less than 15%). Glucuronidation rates are presented as measured initial rates in $\text{nmol}\cdot\text{min}^{-1}\cdot\text{mg}^{-1}$ protein of UGT1A9-enriched insect cells membranes. The derived kinetic constants are presented in Table 3. The Eadie-Hofstee transforms of the data, both from the perspectives of 4-MUG (A) and of UDP (B), are presented in the panels on the right.

Figure 6. Inhibition of the UGT1A9-catalyzed 4-MU glucuronidation reaction by UDP (A) and by 1-naphthol (B). The reactions were carried out in the presence of 0.1% BSA and the points represent the average of two samples (variation between two replicates was less than 15%). The glucuronidation rates are presented as measured initial rates in $\text{nmol}\cdot\text{min}^{-1}\cdot\text{mg}^{-1}$ of UGT1A9-enriched insect cells membranes. The derived kinetic and inhibition constants are presented in Table 4. The Lineweaver-Burk transforms of the data are presented in panels A1 and B1.

Figure 7. Inhibition of the UDPGA kinetics of the UGT1A9-catalyzed 4-MU glucuronidation by UDP (A) and by 1-naphthol (B). The reactions were carried out in the presence of 0.1% BSA and the points represent the average of two samples (variation between two replicates was less than 15%). The glucuronidation rates are presented as measured initial rates in $\text{nmol}\cdot\text{min}^{-1}\cdot\text{mg}^{-1}$ of UGT1A9-enriched insect cells membranes. The derived kinetic and inhibition constants are presented in Table 4. The Lineweaver-Burk transforms of the data are presented in panels A1 and B1.

Figure 8. The proposed enzyme kinetic mechanism of the UGT1A9-catalyzed 4-MU glucuronidation reaction (see *Discussion* for details). The letter symbols represent: E = enzyme (UGT1A9); AX = UDP- α -D-glucuronic acid; A = UDP; B = aglycone substrate (4-MU); I_1 and I_2 = tentative inhibitors that can be removed by BSA. The relative magnitude of the individual rate constants are presented in Table 5.

Tables

Table 1. Previous studies that described the enzyme kinetic mechanism of UGT enzymes.

Enzyme source	Aglycone substrate	Reaction mechanism	Reference
Guinea-pig liver microsomes	Bilirubin	Compulsory-order ternary-complex (UDPGA first, aglycone second) or <i>iso</i> -Theorell-Chance	(Potrepka and Spratt, 1972)
Beef and guinea pig liver microsomes	<i>p</i> -Nitrophenol	Rapid equilibrium random-order ternary complex	(Vessey and Zakim, 1972)
Rat liver microsomes	Morphine	Compulsory-order ternary complex (UDPGA first, aglycone second)	(Sanchez and Tephly, 1975)
Pig kidney microsomes	Estrone	Ternary-complex mechanism, <i>iso</i> -Theorell-Chance (aglycone first, UDPGA second)	(Rao et al., 1976)
Purified UGT from rat liver	Chenodeoxycholic acid and testosterone	Ternary-complex mechanism	(Matern et al., 1982)
Rat intestinal microsomes	1-Naphthol	Compulsory-order ternary-complex (aglycone first, UDPGA second)	(Koster and Noordhoek, 1983)
Two purified UGTs from rat liver	Androsterone and testosterone	Rapid equilibrium random-order ternary-complex	(Falany et al., 1987)
Purified UGT from human liver	Hyodeoxycholic acid	Ternary-complex mechanism	(Matern et al., 1991)
Purified UGT from rat liver microsomes	Substituted phenols	Random-order ternary-complex	(Yin et al., 1994)
Recombinant human UGTs from 1A family	Entacapone, scopoletin, umbelliferone, 1-naphthol, 4-hydroxyestrone, ethinylestradiol	Compulsory-order ternary-complex (UDPGA first, aglycone second)	(Luukkanen et al., 2005)
Recombinant human UGT1A6	Scopoletin	Compulsory-order ternary-complex (UDPGA first, aglycone second)	(Patana et al., 2007)

Table 2. The details of the analytical conditions used for separation and quantification of analytes.

Analyte	Instrument	Eluents and gradient	Injection	Detection	Retention	Quantification
			volume <i>μL</i>	wavelength, <i>nm</i>	time <i>min</i>	Standard curve
4-MU-β-D-glucuronide	HPLC	A: 0.1% Formic acid; B: Acetonitrile 0–3 min, 20→50% B; 3–3.1 min, 50→20% B; 3.1–5 min, 20% B	5–40	Fluorescence, λ_{ex} 316, λ_{em} 382	3.33	Authentic standard
		A: 0.1% Formic acid; B: Acetonitrile 0–3 min, 20→50% B; 3–3.1 min, 50→20% B; 3.1–5 min, 20% B	5–40	Fluorescence, λ_{ex} 325, λ_{em} 450	3.81	Authentic standard
Entacapone	HPLC	A: 0.1% Formic acid; B: Acetonitrile Isocratic, 3 min, 60% B	30	UV, 306 (ref. 450)	1.63	Authentic standard
1-Naphthol-β-D-glucuronide	HPLC	A: 0.1% Formic acid; B: Acetonitrile Isocratic, 6 min, 35% acetonitrile	50	Fluorescence, λ_{ex} 282, λ_{em} 335	2.48	Authentic standard
1-Naphthol	HPLC	A: 0.1% Formic acid; B: Acetonitrile Isocratic, 3 min, 57% acetonitrile	50	Fluorescence, λ_{ex} 291, λ_{em} 460	2.60	Authentic standard

Table 3. The bisubstrate enzyme kinetic parameters of 4-MU glucuronidation by UGT1A9. The data was interpreted by compulsory-order ternary-complex mechanism based on steady-state assumption (eqs. 7 and 8). The values represent a best-fit result \pm S.E. The calculated 95% CI are presented in the parenthesis. The reaction velocity is given per mg of total protein in UGT1A9-enriched insect cell membranes. See *Materials and Methods* for additional details.

Bisubstrate enzyme kinetics parameters of 4-MU glucuronidation by UGT1A9						
Conditions	V_{\max}	K_m (4-MU)	K_m (UDPGA)	K_i (UDPGA)	K_{si} (4-MU)	Kinetic Model
	$nmol \cdot min^{-1} \cdot mg^{-1}$	μM	μM	μM	μM	(r^2)
No BSA	1.25 ± 0.04 (1.18–1.33)	12.0 ± 1.1 (9.86–14.2)	36.3 ± 8.7 (18.7–53.9)	136 ± 26 (83.2–188)	—	Eq. 7 (0.99)
0.1% BSA	9.47 ± 0.13 (9.20–9.75)	2.91 ± 0.16 (2.59–3.24)	90.2 ± 8.6 (72.8–108)	445 ± 46 (352–538)	—	Eq. 7 (0.99)
0.1% BSA with substrate inhibition	9.44 ± 0.19 (9.06–9.83)	3.08 ± 0.22 (2.65–3.52)	64.1 ± 5.4 (53.4–74.8)	574 ± 60 (454–694)	146 ± 8 (130–162)	Eq. 8 (0.99)
0.1% BSA reverse reaction	0.872 ± 0.023 (0.826–0.918)	K_m (4-MUG) 1339 ± 133 (1071–1607)	K_m (UDP) 2.48 ± 0.66 (1.23–4.86)	K_i (UDP) 51.0 ± 9.7 (31.3–70.6)	—	Eq. 7 (0.99)

Table 4. The inhibition parameters of UGT1A9-catalyzed 4-MU glucuronidation in the presence of 0.1% BSA. The values represent a best-fit result \pm S.E. The calculated 95% CI are presented in the parenthesis. The reaction velocity is given per mg of total protein in UGT1A9-enriched insect cell membranes. See *Materials and Methods* for additional details.

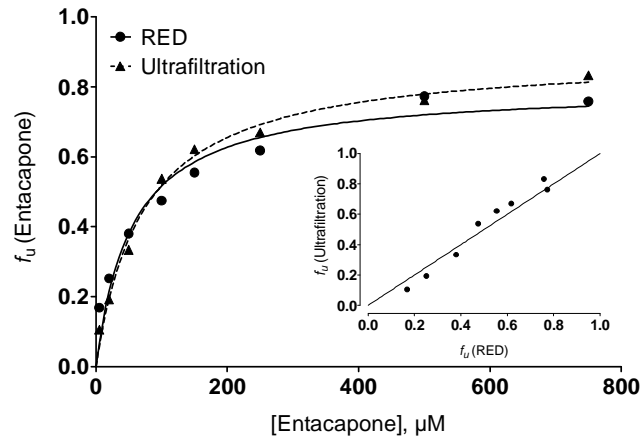
UGT1A9 inhibition studies in the presence of 0.1% BSA								
Variable substrate	Fixed substrate (concentration)	Inhibitor	Type of inhibition	K_m	V_{max}	K_i	α	Goodness-of-fit
	μM			μM	$nmol \cdot min^{-1} \cdot mg^{-1}$	μM		(r^2)
4-MU	UDPGA (2000)	UDP	Mixed	2.97 ± 0.14 (2.68–3.26)	9.56 ± 0.11 (9.33–9.79)	121 ± 12 (98.1–145)	2.92 ± 0.43 (2.07–3.77)	0.99
4-MU	UDPGA (2000)	1-Naphthol	Mixed	3.20 ± 0.25 (2.71–3.69)	7.73 ± 0.16 (7.43–8.04)	0.0198 ± 0.0027 (0.0153–0.0243)	7.38 ± 1.75 (3.91–10.9)	0.98
UDPGA	4-MU (30)	UDP	Competitive	117 ± 5 (107–126)	8.78 ± 0.08 (8.62–8.93)	19.1 ± 0.8 (17.5–20.6)	—	0.99
UDPGA	4-MU (30)	1-Naphthol	Uncompetitive	137 ± 5 (127–147)	9.10 ± 0.09 (8.93–9.28)	0.0658 ± 0.0015 (0.0628–0.0689)	—	0.99

Table 5. The relative individual rate constants for compulsory-order ternary-complex mechanism of UGT1A9-catalyzed 4-MU glucuronidation. The different rate constants were normalized to the arbitrarily set value: $V_{max}^f = k_{cat}^f[E] = 1$. The superscripts *f* and *r* indicate the forward and the reverse reaction, respectively.

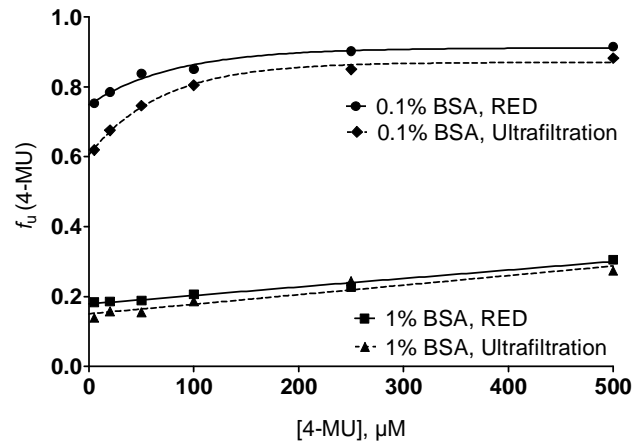
Individual rate constants of UGT1A9-catalyzed 4-MU glucuronidation in the presence of 0.1% BSA		
Rate constant equation	Relative value, normalized to $k_{cat}^f[E] = 1$	Order of rate constant
$k_1[E] = \frac{V_{max}^f}{K_{mAX}}$	0.011	second-order
$k_{-1}[E] = \frac{V_{max}^f K_{iAX}}{K_{mAX}}$	4.930	first-order
$k_2[E] = \frac{V_{max}^f(k_{-2} + k_3)}{k_3 + K_{mB}}$	0.359	second-order
$k_{-2}[E] = \frac{V_{max}^f V_{max}^r K_{iAX}}{V_{max}^f K_{iAX} - V_{max}^r K_{mAX}}$	0.094	first-order
$k_3[E] = \frac{V_{max}^f V_{max}^r K_{iA}}{V_{max}^r K_{iA} - V_{max}^f K_{mA}}$	2.126	first-order
$k_{-3}[E] = \frac{V_{max}^r(k_{-2} + k_3)}{k_{-2} K_{mBX}}$	0.002	second-order
$k_4[E] = \frac{V_{max}^r K_{iA}}{K_{mA}}$	1.888	first-order
$k_{-4}[E] = \frac{V_{max}^r}{K_{mA}}$	0.037	second-order
$k_{cat}^f[E] = V_{max}^f = \frac{k_3 k_4}{k_3 + k_4}$	1.000	first-order
$k_{cat}^r[E] = V_{max}^r = \frac{k_{-1} k_{-2}}{k_{-1} + k_{-2}}$	0.092	first-order

Figure 1.

A: Entacapone binding to 0.1% BSA, correlation between RED and ultrafiltration



B: 4-MU binding to 0.1 and 1% BSA, correlation between RED and ultrafiltration



C: 1-Naphthol binding to 0.1% BSA, RED

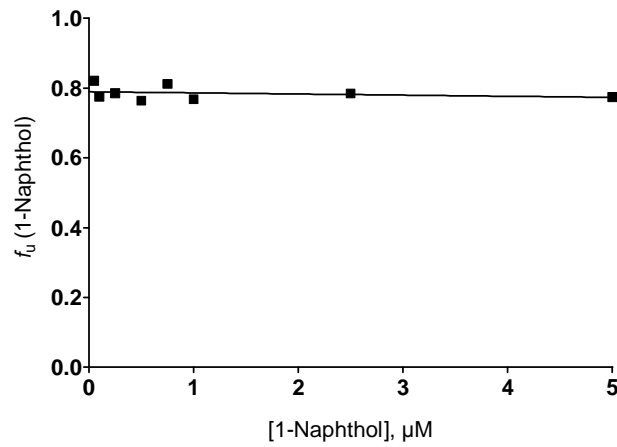


Figure 2.

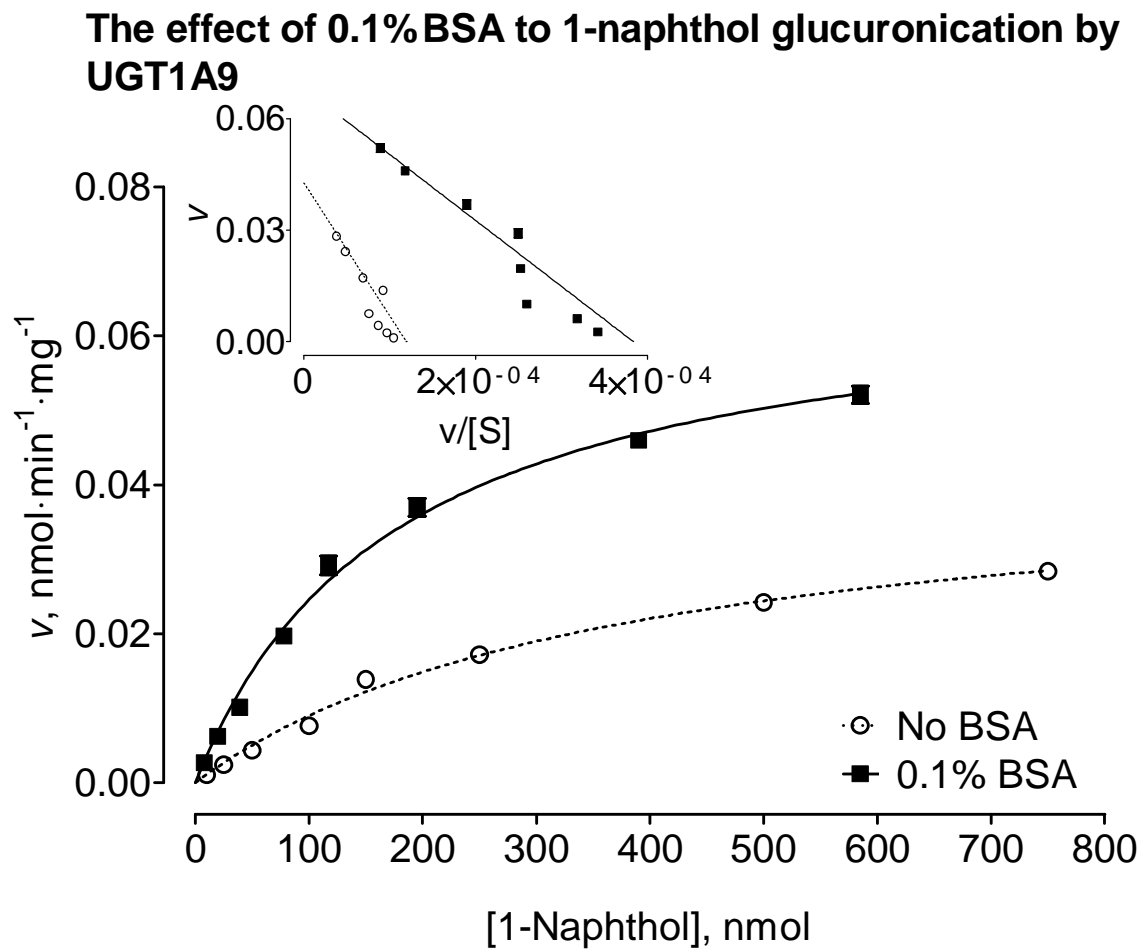


Figure 3.

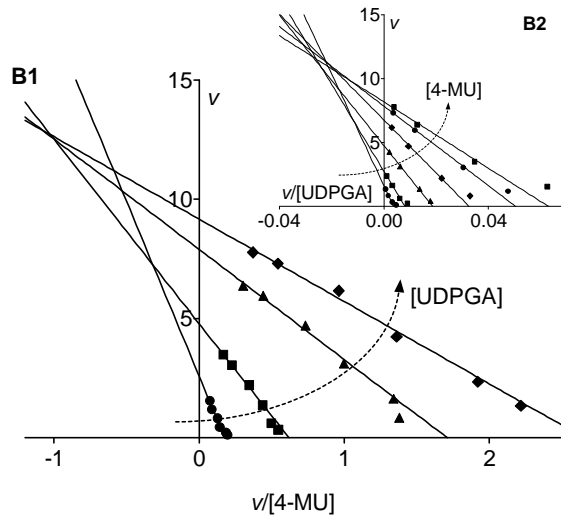
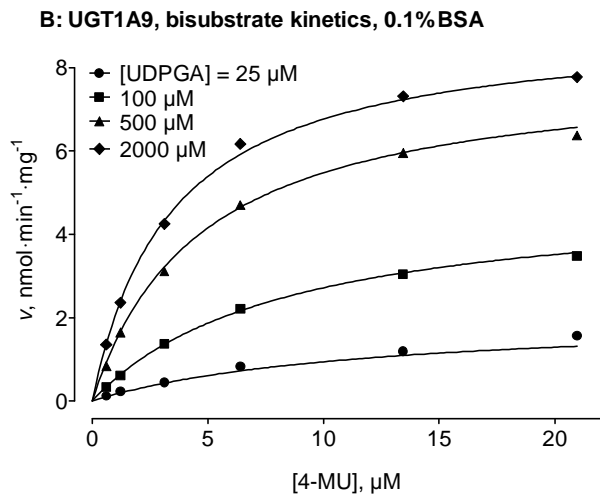
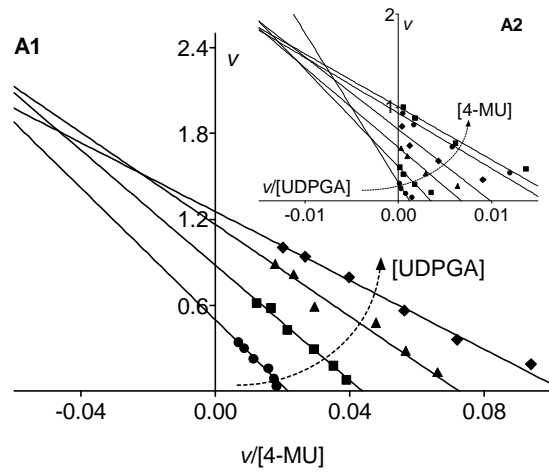
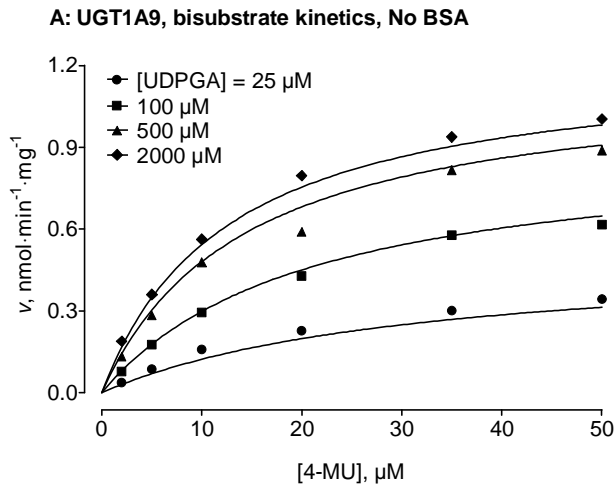


Figure 4.

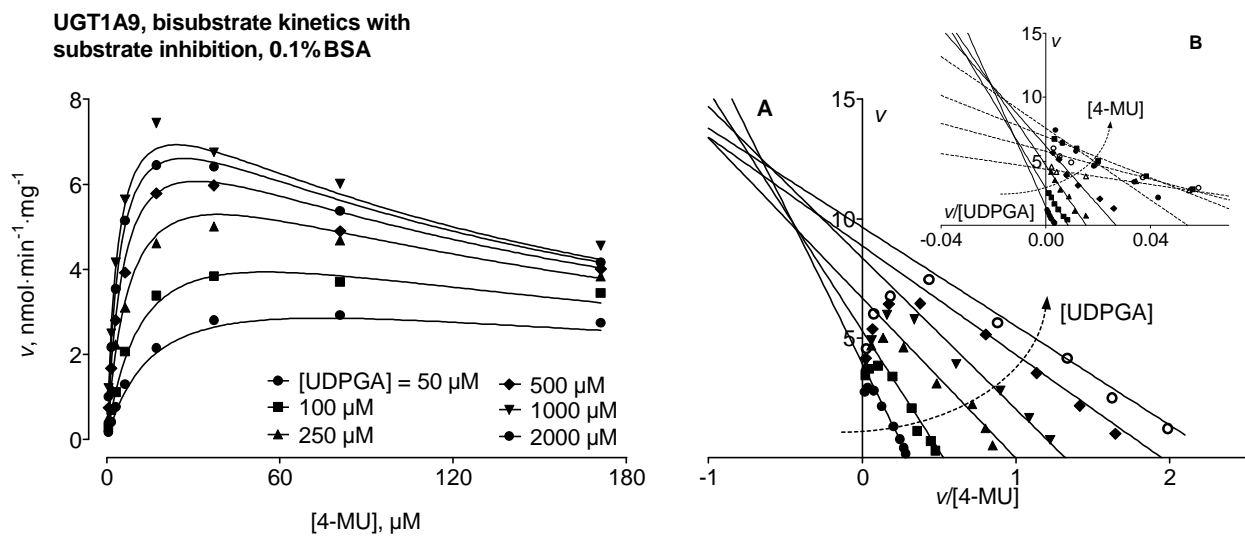


Figure 5.

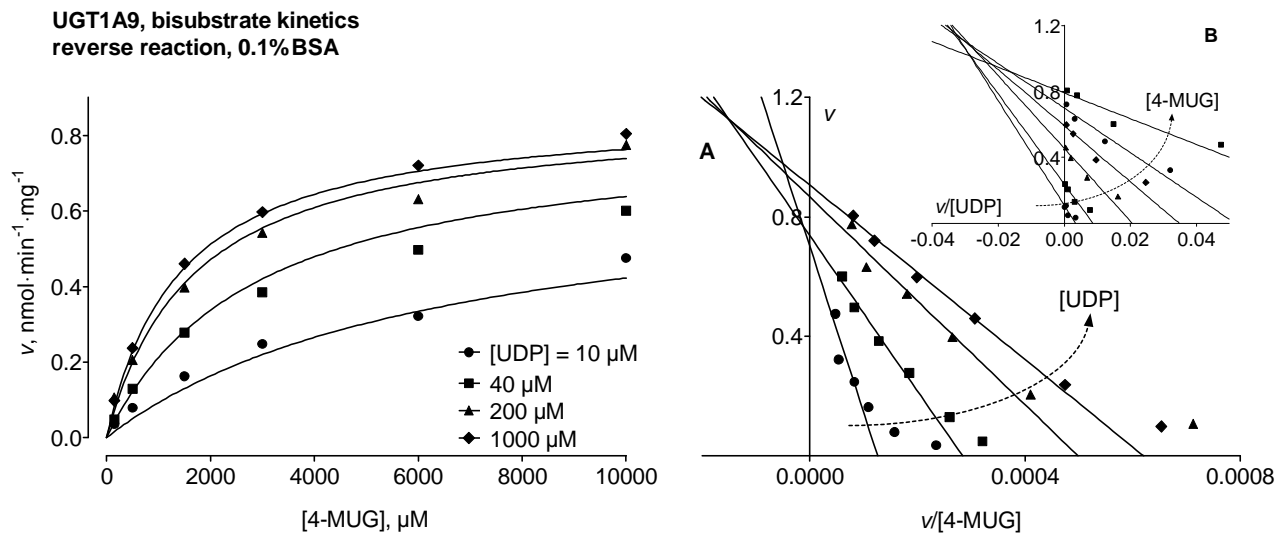
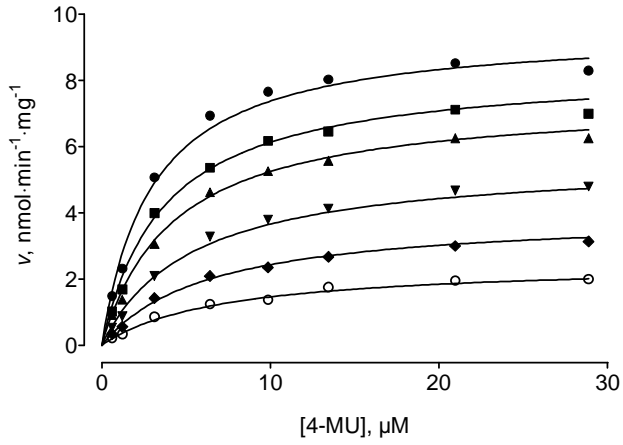
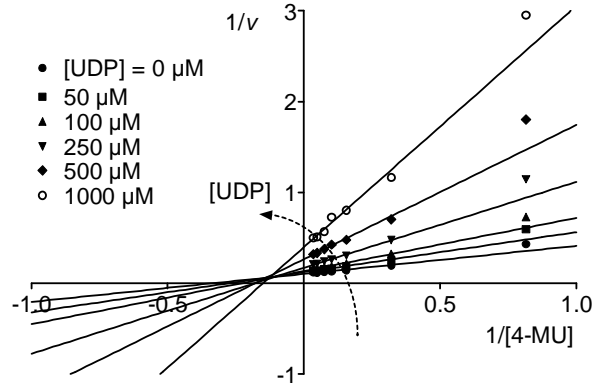


Figure 6.

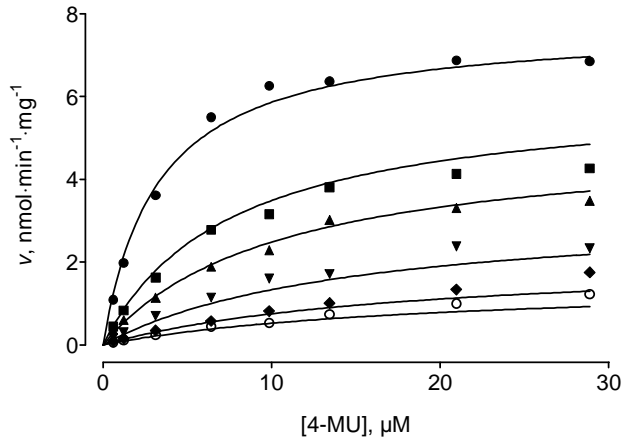
A: 4-MU kinetics in the presence of 0.1% BSA, inhibition by UDP



A1



B: 4-MU kinetics in the presence of 0.1% BSA, inhibition by 1-naphthol



B1

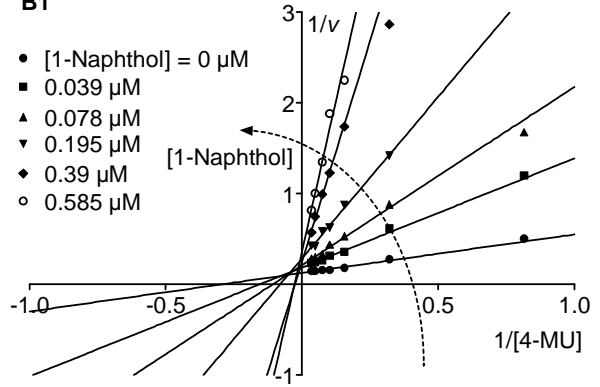
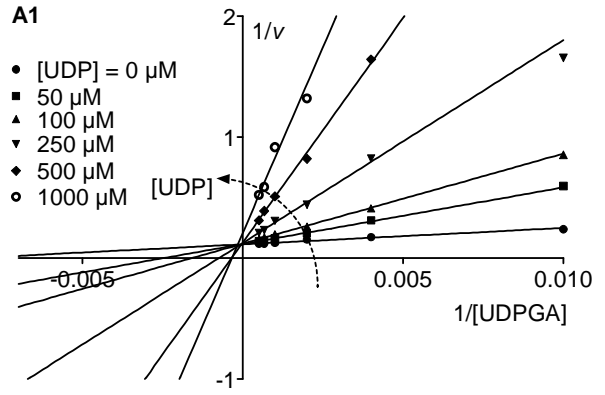
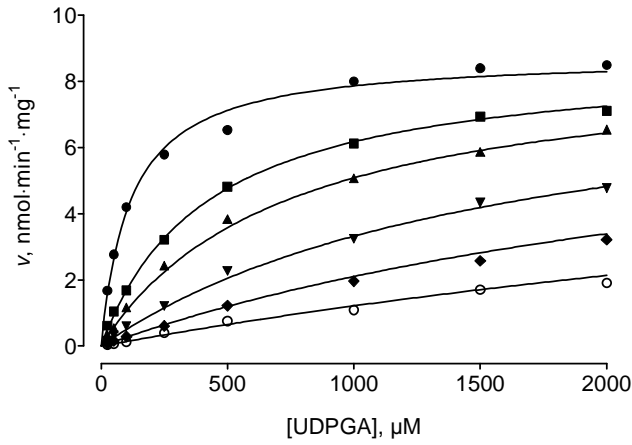


Figure 7.

A: UDPGA kinetics in the presence of 0.1% BSA, inhibition by UDP



B: UDPGA kinetics in the presence of 0.1% BSA, inhibition by 1-naphthol

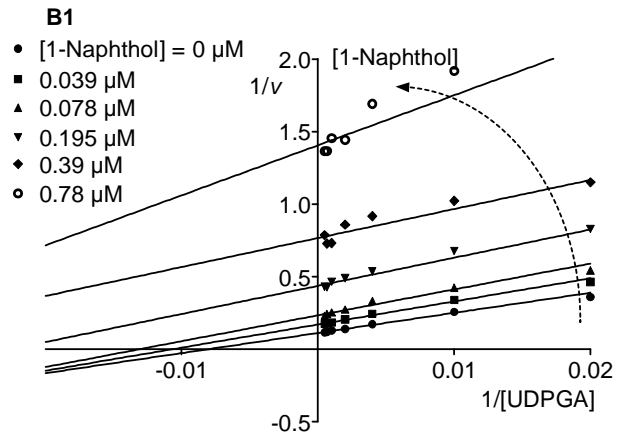
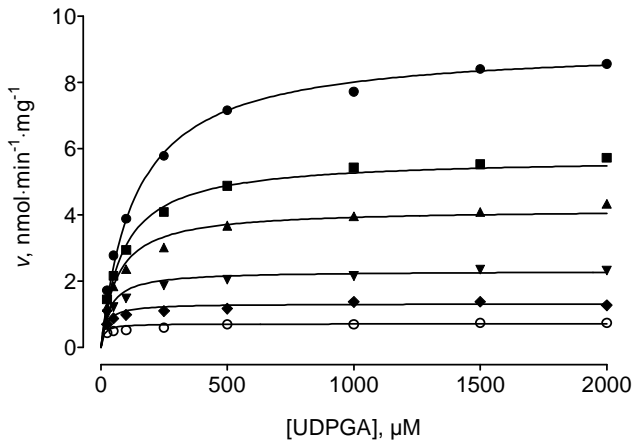


Figure 8.

